

EMITTANCE PRESERVATION FOR THE CURVED ILC MAIN LINAC *

Kirti Ranjan[#], Nikolay Solyak, Shekhar Mishra, Jean-Francois Ostiguy, Alexander Valishev,
Fermi National Accelerator Laboratory (FNAL), Batavia IL 60510, U.S.A.

Peter Tenenbaum, Stanford Linear Accelerator Center (SLAC), Menlo Park, CA 94025, U.S.A.

Abstract

We present here the simulation results on the emittance dilution in the curved International Linear Collider (ILC) main linac using Dispersion Free Steering (DFS) under the nominal misalignments of the beamline components. In order to understand the implication of the earth's curvature on beam dynamics, we present the comparison of the curved linac with the laser straight geometry. We have studied the sensitivity of DFS to various misalignments and have also considered the effect of incorporating incoming beam jitter and quadrupole vibration jitter. In addition, the robustness of DFS to the failure of a corrector magnet or Beam Position Monitor (BPM) is investigated. The beneficial effect of dispersion bumps on the emittance dilution performance is also discussed.

INTRODUCTION

One of the crucial accelerator design and operation issues for the proposed ILC machine would be the preservation of small transverse beam emittances in beam propagation through main linac. Because of the large aspect ratio in both spot size and emittance, challenges in the vertical plane would be at least an order of magnitude more difficult than in the horizontal plane. Thus in this work only emittance preservation in the vertical plane is considered. Various sources of emittance dilution in the main linac include dispersion originating from misaligned quadrupoles and BPMs, pitched cavities and cryomodules, wakefields generated from cavity offsets, and coupling between the transverse planes coming from rotated (or skew) quads. It is well established now that beam-based alignment (BBA) techniques in the main linac will be indispensable to limit the emittance growth to the desired small values. To this end, various static tuning algorithms were proposed, investigated, and developed over the last 15 years [1]. Dispersion Free Steering (DFS) was demonstrated to be one of the effective techniques in earlier NLC [2] and TESLA [3] studies and is also considered to be an attractive approach for the ILC main linac. However, almost all earlier studies assumed a laser-straight geometry of the main linac. Based on some recent studies [4], it is envisaged in the ILC Baseline Configuration Document (BCD) [5] that unless beam dynamics studies or site-specific reasons dictate otherwise, the ILC main linac will follow the earth's curvature. It is thus important to analyze the performance of DFS in a curved linac. In order to understand the stringency of the tolerance of a given

beamline element it is crucial to study the sensitivity of the DFS algorithm to various misalignments and incoming beam and quad vibration jitter. The robustness of the DFS algorithm to a failure of a BPM or corrector is also considered. Finally, we have examined the effect of incorporating dispersion bumps in the ILC main linac.

ILC MAIN LINAC

The ILC main linac considered in this study is an adaptation from the design envisaged in the ILC BCD. A fully loaded gradient of 31.5 MeV/m is considered for the 9-cell 1.3 GHz accelerating cavities. The main linac cryogenic system is divided into cryomodules (CM), with 8 cavities per CM. A quad package consisting of a quadrupole magnet, a cavity-style BPM, and horizontal and vertical corrector magnets is installed in every fourth CM. The magnet optics is a FODO lattice with a phase advance per cell of 75° (60°) in the horizontal (vertical) plane. The beam injection energy is 15 GeV, the extraction energy is 250 GeV, and the single bunch charge is 2×10^{10} . The nominal installation precision for various beamline elements are given in Table 1.

Table 1: RMS alignment tolerances for a curved ILC main linac in the vertical plane.

Misalignment	With respect to	Tolerance (μm)
Quad offset	CM	300
Quad rotation	CM	300
BPM resolution	-	1
BPM offset	CM	300
Cavity offset	CM	300
Cavity pitch	CM	300
CM offset	Survey Line	200
CM pitch	Survey Line	20

Simulations are performed using MatLIAR [6]. In order to simulate the effect of the earth's curvature in MatLIAR, each successive CM was tilted by a vertical half-angle of $0.84 \mu\text{rad}$ with respect to the previous CM. The beam is launched onto the design curved orbit using the vertical correctors. Because of the location of a corrector only in every fourth CM, there exists a systematic beam offset of maximum $40 \mu\text{m}$ through the cavities, but its effect is small compared to the misalignment tolerances of the cavities and CM (see Table 1). The curved geometry also results in a finite vertical "design" dispersion of about 1mm in the linac, which must be matched to the incoming beam to prevent beam filamentation.

*Work supported by U.S. Department of Energy

[#]kirti@fnal.gov

DFS IMPLEMENTATION

After incorporating the nominal misalignments, one-to-one steering is applied in which the beam is steered, using the vertical corrector magnets, to the center of each BPM. However, this correction scheme is sensitive to BPM-to-quad offsets resulting in dispersive emittance growth.

DFS is one of the steering algorithms which, as the name suggests, is designed to minimize dispersion and is independent of the BPM-to-quad offsets. For its implementation, the linac is divided into a number of alignment segments with about 40 quads per segment. There is a 50% overlap between segments. The BPMs are used to measure two orbits in each segment. The first orbit is measured under nominal conditions while the second orbit is measured by switching off some RF cavities upstream of the segment. Three BPMs upstream of each segment are used for fitting the incoming trajectory. The maximum energy change for a given segment is chosen to be 20% of the nominal beam energy at the upstream end or 18 GeV, whichever is smaller. It should be noted that the first few quads cannot be aligned by DFS as there are no RF stations upstream of that segment. Thus, we assumed a smaller BPM offset of 30 μm RMS with respect to survey line for the first seven BPMs.

The correction is weighted to simultaneously minimize the measured dispersion and the RMS value of the BPM readings; the weight ratio of the constraints is chosen to be $\sqrt{2}$ times the ratio of the BPM resolution to the BPM offset. The correction is applied using the corrector magnets.

RESULTS

Figure 1 shows the projected normalized emittance growth in vertical plane for a curve ILC linac without any misalignment. Also shown is the corrected emittance growth which is calculated after removing the contribution from the design dispersion. An almost negligible corrected emittance growth of ~ 0.2 nm is observed in the ILC linac.

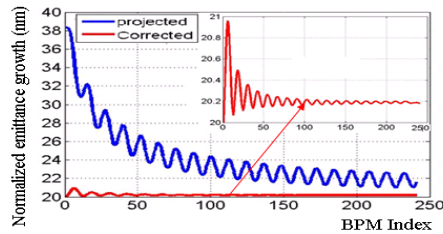


Figure 1: Projected emittance growth (blue) and design dispersion corrected projected emittance growth (red) in curve ILC main linac without any misalignment. Inset shows the blown up region for the design dispersion corrected emittance growth.

Figure 2 shows the mean corrected projected emittance growth for 50 random individual machines after incorporating the misalignments given in Table 1 and applying DFS, for both the curved and laser-straight

geometry. The same DFS parameters were used in both cases. Figure 2 also shows the corrected emittance dilution distribution for 50 individual machines. It is evident that the emittance growth in a curved linac is very similar to the emittance growth in a straight linac.

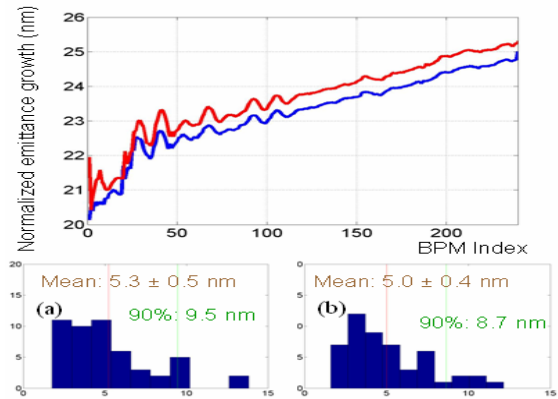


Figure 2: The top plot compares the mean (of 50 random machines) corrected emittance growth for a curved ILC linac (red) and a laser-straight linac (blue) after DFS. The bottom plots show the corrected emittance growth for 50 individual linacs with (a) a curved geometry and (b) a laser-straight geometry.

The sensitivity of the emittance dilution for DFS is investigated for conditions different from the nominal one. Keeping all other misalignments at their nominal values, a given misalignment value is varied and its effect on the emittance dilution of a curved ILC linac is studied. Figure 3 shows that DFS is most sensitive to variations of BPM resolution, cavity pitch, CM offset and quad roll. DFS is found to be almost independent of variations in BPM offset, quad offset, cavity offset, and CM pitch. It is also observed that the DFS algorithm is less sensitive to variations of incoming beam jitter as compared to white-noise quad vibration jitter (Figure 4).

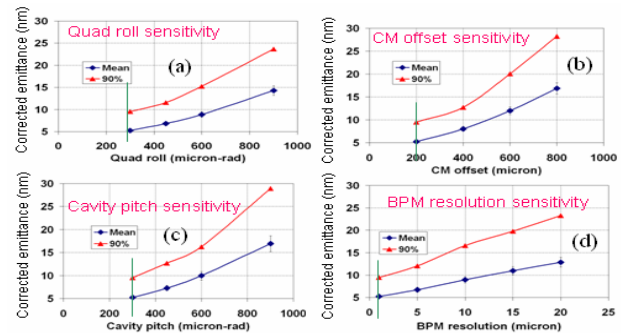


Figure 3: Mean and 90% corrected emittance growth in the ILC curved linac after DFS for different sets of misalignments.

Table 2 shows the contribution of three individual sources (dispersion, wakefield, and x-y coupling) to the nominal corrected emittance dilution after DFS for a curved ILC main linac. For the wakefield case only cavity offsets are included, for x-y coupling only quad roll is

included, and for the dispersion case only quad and BPM offsets and cavity and CM pitches are considered.

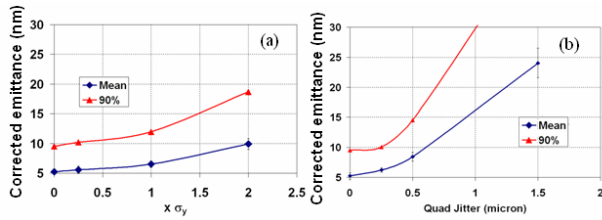


Figure 4: Mean (Blue) and 90% (Red) corrected emittance growth in the curved ILC linac after DFS for 50 random machines as a function of (a) incoming y and y' beam jitter and (b) quad vibration jitter (in μm).

Table 2: Contribution to the nominal corrected emittance dilution from individual sources in a curved ILC linac.

Source	Mean dilution (nm)	90% dilution (nm)
Dispersion	1.99 ± 0.24	4.22
Wakefield	1.8 ± 0.17	3
Coupling	1.47 ± 0.13	2.83

The effect of a random failed BPM on the DFS algorithm is shown in Figure 5. It is assumed that the faulty BPM, randomly chosen as the 50th, reads zero throughout. Figure 5(a) illustrates that if the faulty BPM is used in the correction then it will deteriorate the performance of the DFS. However, if the faulty BPM can be located and excluded from the correction (Figure 5(b)), then the nominal DFS performance is recovered.

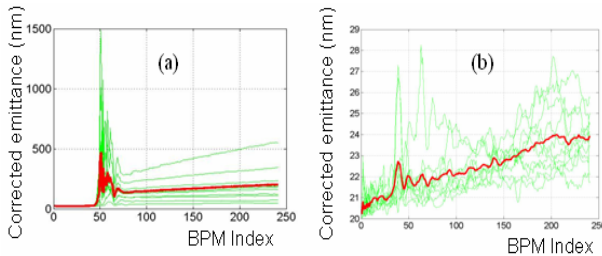


Figure 5: Corrected emittance growth in the ILC main linac for 10 random machines (green) and their mean (red) when (a) a faulty BPM is used in DFS and (b) the faulty BPM is not used in DFS.

Since each of the vertical corrector magnets is used to steer the beam on the design curved orbit, failure of even a single corrector results in a large orbit oscillation ($\sim 500 \mu\text{m}$) and very large emittance dilution even in an otherwise perfect linac. In order to assess the effect of the failure of a corrector, we assumed that the two neighboring correctors of a failed corrector (one upstream and one downstream) can be used to steer the beam on the design orbit. It was found that if we can locate the failed corrector and exclude it from DFS then the emittance growth in the main linac is similar to that in a linac without a corrector failure. Figure 6 shows that the

emittance dilution after DFS increases only slightly even in the case of a failure of 5 random correctors, assuming that the failed correctors can be excluded from the correction algorithm.

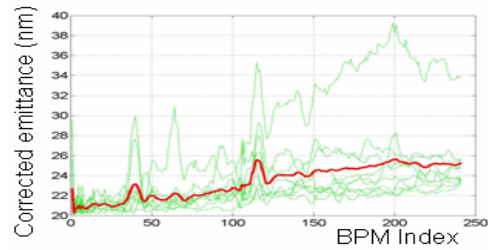


Figure 6: Corrected emittance growth in the ILC main linac for 10 random machines (green) and their mean (red) when there are 5 randomly placed failed correctors in the linac, but excluded from the correction schemes.

Dispersion bumps [7] are also considered as an effective means of limiting the emittance dilution in a linac. Dispersion bumps in ILC main linac are incorporated by having two sets of correctors 90° apart in betatron phase, each set consisting of two correctors 180° apart. The corrector fields are then varied and the beam size near the end of the main linac is measured with two wire scanners placed 90° apart (with 2% resolution assumed for the beam size measurement). Figure 7 shows that there is a significant reduction in emittance dilution by using such a bump after DFS in a curved ILC main linac.

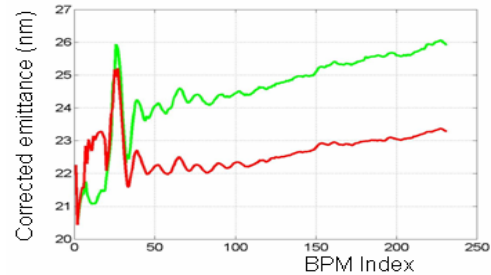


Figure 7: Mean corrected emittance growth in a curved ILC main linac for 40 random machines after DFS (green) and then using dispersion bump (red).

It should be noted that the final realistic design considering full details of the ILC main linac is ongoing, and the preliminary studies on DFS give comparable results with the work presented here.

REFERENCES

- [1] T. Raubenheimer and P. Tenenbaum, LCC-0129, LCC Tech. Notes, 2003
- [2] P. Tenenbaum, LCC-0071, LCC Tech. Notes, 2001.
- [3] P. Tenenbaum, R. Brinkmann and V. Tsakanov EPAC'02, Paris, 2002, p. 515.
- [4] N. Walker, EUROTeV-Report-2005-017, 2005.
- [5] http://www.linearcollider.org/wiki/doku.php?id=bcd:bcd_home
- [6] <http://www.slac.stanford.edu/accel/nlc/local/AccelPhysics/codes/liar/web/liar.htm>
- [7] P. Tenenbaum, LCC-0138, LCC Tech. Notes, 2004.